Eur. Phys. J. D (2021) 75:314
https://doi.org/10.1140/epjd/s10053-021-00316-z

THE EUROPEAN PHYSICAL JOURNAL D

Regular Article Atomic and Molecular Collisions

Effect of thermochemical treatments on laser-induced luminescence spectra from strontium titanate: comparison with swift ion-beam irradiation experiments

M. L. Crespillo[1,2,a], J. T. Graham[3], F. Agulló-López[1], Y. Zhang[4], and W. J. Weber[2,4,b]

[1] Centro de Microanálisis de Materiales, CMAM-UAM, 28049 Cantoblanco, Madrid, Spain
[2] Department of Materials Science and Engineering, University of Tennessee, Knoxville, TN 37996, USA
[3] Department of Nuclear Engineering and Radiation Science, Missouri University of Science and Technology, Rolla, MO 65409, USA
[4] Materials Science and Technology Division, Oak Ridge National Laboratory, Oak Ridge, TN 37831, USA

Received 6 July 2021 / Accepted 29 November 2021 / Published online 28 December 2021

Abstract. Results recently reported on the effect of thermochemical treatments on the (He-Cd) laser-excited emission spectra of strontium titanate (STO) are re-analyzed here and compared with results obtained under ion-beam irradiation. Contributing bands centered at 2.4 eV and 2.8 eV, which appear under laser excitation, present intensities dependent upon previous thermal treatments in oxidizing (O_2) or reducing atmosphere (H_2). As a key result, the emission band centered at 2.8 eV is clearly enhanced in samples exposed to a reducing atmosphere. From a comparison with the ionoluminescence data, it is concluded that the laser-excited experiments can be rationalized within a framework developed from ion-beam excitation studies. In particular, the band at 2.8 eV, sometimes attributed to oxygen vacancies, behaves as expected for optical transitions from conduction-band (CB) states to the ground state level of the self-trapped exciton center. The band at 2.0 eV reported in ion-beam irradiated STO, and attributed to oxygen vacancies, is not observed in laser-excited crystals. As a consequence of our analysis, a consistent scheme of electronic energy levels and optical transitions can now be reliably offered for strontium titanate.

1 Introduction

Strontium titanate ($SrTiO_3$, STO) is a paradigmatic example of a class of oxide perovskites with outstanding optoelectronic properties and is a dominant material in the novel field of complex-oxide-based electronics [1, 2]. Having a simple cubic structure at room temperature (RT) and an indirect band gap of 3.27 eV [3], it presents a rich variety of electrical properties ranging from insulating to metallic [4], semiconducting and even superconducting behavior [5]. Moreover, under suitable doping, it shows efficient photocatalytic activity for hydrogen generation through water decomposition [6–8]. For each of these noteworthy behaviors, structural and impurity defects are known to play a key role [9]. In particular, oxygen vacancies are intrinsic defects that determine many of the physical and chemical properties of oxide perovskites, especially in STO. Luminescence, due to its superior sensitivity and resolution, is the main, and often only optical technique used to investigate the properties of transition metal impurities and defects in dielectric materials and their relation to the lattice structure. Photoluminescence (PL), as a key optical technique, is widely used to identify and characterize excited states of defect centers [10, 11].

Recently, some interesting results on the effect of thermal treatments in different atmospheres on the emission spectra of STO have been reported for a broad range of temperatures from 10 K to RT [11]. Although this work from Lim et al. [11] focused on the main emission band centered at 2.6 eV, the paper presented evidence that nearby bands at 2.4 eV and 2.8 eV were quite sensitive to the thermochemical environment. The data were obtained under excitation above the bandgap using a He-Cd laser (325 nm). The role of several oxidation–reduction treatments at temperatures ranging from 400 to 900 °C was investigated. The obtained results showed that the relative yields of the bands at 2.4 eV and 2.8 eV could be significantly modified by subjecting the samples to either oxidizing (O_2 atmosphere) or reducing (H_2 atmosphere) thermal treatments. In particular, the intriguing emission at 2.8 eV was clearly enhanced in the samples that had been heated in a reducing atmosphere. In this work, we discuss the above data in relation to extensive and systematic information gathered under ion-beam irradiation [8, 12–16]. This procedure induces electronic excitation above the bandgap, as achieved by laser excitation, but offers additional possibilities, including the generation

[a] e-mail: miguel.crespillo@uam.es (corresponding author)
[b] e-mail: wjweber@utk.edu (corresponding author)

of oxygen vacancies through elastic ion-atom collisions. A major experimental advantage of this approach is that the irradiation parameters (energy and range of the projectile particles) can be easily modified and, therefore, the deposited energy and the effects of the damage can be tailored. The excitation intensity can reach local electronic densities comparable to femtosecond pulsed lasers ($\sim 10^{19}$–10^{21} cm^{-3}), which enables one to investigate the role of electronic excitation density on light emissions. Finally, the broad excitation spectrum and high electron–hole densities guarantee the simultaneous observation of all contributing luminescence bands and interplay among them [16, 17]. The results obtained with ion-beam-induced luminescence or ionoluminescence (*IL*) have provided a coherent framework to account for the radiative emission mechanisms by electronic de-excitation [14].

The objective of this paper consists of discussing the newly reported data on laser excitation [11] in relation to those recently presented in our ion-beam excitation (ionoluminescence) studies [8, 12–16]. Using ions with different masses (from H to Ti) and energies up to 18 MeV, the ionoluminescence (*IL*) studies led to a physical model that accounts for most experimental features of the light emissions in ion-beam irradiated STO crystals. Moreover, they revealed that *isolated* oxygen vacancies are responsible for the emission band centered at 2.0 eV. In fact, a linear correlation was found between the initial growth rate of the red emission band at 2.0 eV and the generation rate of oxygen vacancies per incident ion, as calculated using the SRIM Monte Carlo code [18, 19]. Additional studies have associated the 2.0 eV emission to an optical transition between *d*-levels of the Ti^{3+} electron small-polaron, which is trapped near the oxygen vacancy [13, 14]. The assignment is corroborated by theoretical calculations [20–23] for the *d*-levels of Ti^{3+} around the vacancy. On the other hand, the broad green emission band centered at 2.5 eV, accompanied by strong lattice relaxation, is associated with a triplet-singlet optical transition of a self-trapped exciton (STE) inside a regular octahedron [24–27]. It has been observed under a large variety of excitation methods including visible light, X-rays, and ion beams [25, 26, 28, 29], and the mean lifetime exhibits a long decay time of milliseconds in accordance with the spin-forbidden character of the transition [25, 27, 30]. Finally, more recent results suggest that the blue emission at 2.8 eV is not consistent with a previous assignment to oxygen vacancies [31], and it has been very recently associated with optical transitions from conduction band (CB) states to the ground state of the STE [15].

As we will discuss in this paper, the data reported in [11], after different thermal treatments using both reducing as well as oxidizing atmospheres, appear relevant to address the intriguing origin of those emission bands. In particular, it is shown that the effect of thermal treatments on the emission bands centered at 2.4 eV and 2.8 eV is consistent with the model derived from the ion-beam experiments [12–16], although some unsettled questions may still remain.

2 Experimental details

Along this section, a brief overview of most relevant experimental details from the previous studies is presented with the aim of making a more straightforward comparison between the parameters used in both physical scenarios.

2.1 Experiments with laser excitation

(100) STO single crystals used in [11] were supplied by the Crystal Bank at Pusan National University. Laser excitation, with an energy above the bandgap, was achieved using a continuous He-Cd laser (λ=325 nm) [32]. Unfortunately, Lim et al. [11] did not report the excitation rate to allow for a more quantitative comparison of the electronic excitation densities.

Before the photoluminescence (*PL*) experiments were carried out, crystals were subjected to high temperature annealing treatments in different atmospheres. The annealing temperature was fixed at 900 °C in the reduced crystals treated in H_2 and N_2 atmospheres. For the annealings performed in O_2, the temperature was varied from 400 to 900 °C.

2.2 Experiments with ion-beam irradiation

High-purity, one-side EPI-polished (ultra-flat, surface finish (RMS) lower than 5 Å), stoichiometric $SrTiO_3$ (001) single crystals for the ion-beam studies were obtained from MTI Corporation Ltd. (Richmond, CA). The nominal impurity concentrations, as provided by the manufacturer, can be found elsewhere (Table 1 in [8]). Substrates were irradiated at temperatures of 100 K, 170 K and 300 K (RT) with a variety of projectile ions and energies (3 MeV H, 8 MeV O, 15 MeV Si, 18 MeV Cl and 18 MeV Ti ions) to cover a wide range of electronic (S_e) and nuclear (S_n) stopping powers. A more detailed description of the irradiation setup and experiments can be found elsewhere [8, 12, 13, 15, 33, 34]. The relevant irradiation parameters, including electronic excitation densities and total number of oxygen vacancies generated per incident ion [18], are summarized in Table 1. Typical electronic excitation rates reached under irradiation are around 10^{18} e–h pairs cm^{-2} s^{-1}, comparable to those achieved in most picosecond (ps)-pulsed laser experiments [15, 16].

2.3 SRIM simulations

Electronic stopping powers (S_e), projected ion ranges (R_p), ionization energies (E_{ioniz}), and number of generated oxygen vacancies, included in Table 1, were calculated using the Stopping and Range of Ions in Matter (SRIM) binary collision approximation (BCA) software (version 2012) [18, 19] using full-cascade simulations [35]. Threshold displacement energies of 35.7 eV, 65 eV and 53.5 eV were assumed for the O, Ti, and Sr atoms, respectively [36].

Table 1 Irradiation parameters calculated using SRIM (version 2012) full-cascade simulations [18, 19]. R_p is the projected ion range, $S_{e,\,max}$ is the maximum electronic stopping power and E_{ioniz} is the energy deposited in the electronic system per incident ion. F is the average incident particle flux and ρ_{e-h} is the excited e–h pair density generated per incident ion per unit of volume along R_p assuming an excitation radius of $\sim$ 10 nm (see Refs. [15, 16] for further details). *Total oxygen vacancies* are the total number of oxygen vacancies produced per incident ion integrated along R_p

Ion, Energy (MeV)	R_p (μm)	$S_{e,\,max}$ (keV/nm)	E_{ioniz} (MeV)	F ($\times 10^{12}$ cm^{-2} s^{-1})	ρ_{e-h} (e–h cm^{-3})	Total oxygen vacancies
H, 3	54.00	0.14	2.98	2.20	2.20×10^{19}	11.42
O, 8	3.70	3.21	7.85	0.90	8.55×10^{20}	756.43
Ti, 18	4.15	8.31	17.05	0.44	1.64×10^{21}	4749.95
Cl, 18	4.15	7.31	17.47	0.44	1.68×10^{21}	2816.96
Si, 15	4.00	6.14	14.64	0.64	1.46×10^{21}	2002.95

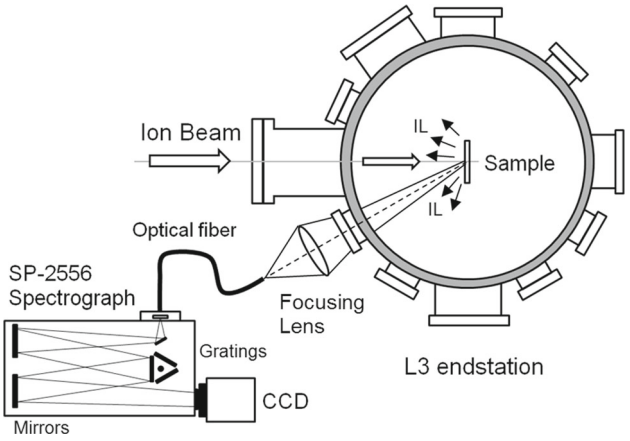

Fig. 1 Schematic of the experimental setup for *in situ* ionoluminescence (*IL*) measurements reprinted from Crespillo et al. [34], Copyright (2016), with permission from Elsevier

2.4 Ionoluminescence (IL) characterization

The experimental setup for *IL* spectra acquisition (used in the previous works by the authors of the present paper in the Ion Beam Materials Laboratory (IBML UTK-ORNL) at the University of Tennessee, Knoxville is schematically illustrated in Fig. 1 and is described in detail elsewhere [8, 12]. The light emitted from the samples is transmitted through a sapphire window and collected into a silica optical fiber of 1 mm diameter located outside the vacuum chamber and coupled to an imaging spectrometer. The spectral resolution is better than 0.2 nm. More details regarding the optical setup, spectrometer and detector can be found in [33, 34]. The sample temperature was monitored during the ion irradiation experiment with a K-type (chromel–alumel) thermocouple attached to the sample surface [33, 37].

3 Comparative analysis between laser-excited (PL) and ionoluminescence (IL) spectra from STO: Physical discussion

Figure 2(a) illustrates the emission spectra observed in [11] consisting of several broad bands with peaks centered at 2.39 eV, 2.57 eV and 2.77 eV, although small shifts can be observed depending on thermal treatments. On the other side, a main conclusion of the *IL* studies performed at UTK [8, 12–16] is that all emission spectra can be decomposed into three nearly Gaussian component bands centered at 2.0 eV (red), 2.5 eV (green) and 2.8 eV (blue). The decomposition, plotted in Fig. 2(b), is quite robust and essentially independent of the type of projectile ion and temperature. For simplicity, only two projectile ions are included in the figure, a light ion (H) and a representative heavy ion (Si). The band centered at 2.0 eV is not observed under laser excitation (see Fig. 2(a)), whereas the bands centered at 2.57 eV and 2.77 eV appear similar under both types of excitation source, laser and ion-beam. Slight differences in the peak centers and widths of the bands are possible due to the shape parameters of those bands being somewhat dependent on temperature and possibly on the specific nature of the substrates (crystal growth method, residual strain, presence of impurities, etc.). In fact, different values for those parameters were found when reviewing the literature (e.g., see Table 1 in Ref. [12]). The spectral decomposition is displayed in Fig. 2(b) at representative temperatures (RT (300 K), 170 K and 100 K). Noteworthy differences between the results obtained under laser excitation [14] and ion-beam irradiation are addressed next.

First, the red band (at 2.0 eV) is very weak and difficult to identify in the spectra from Lim et al. [11]. This is not surprising since our recent *IL* work has conclusively shown that it is associated to oxygen vacancies, and laser irradiation is not expected to generate new vacancies. Similarly, that emission band has

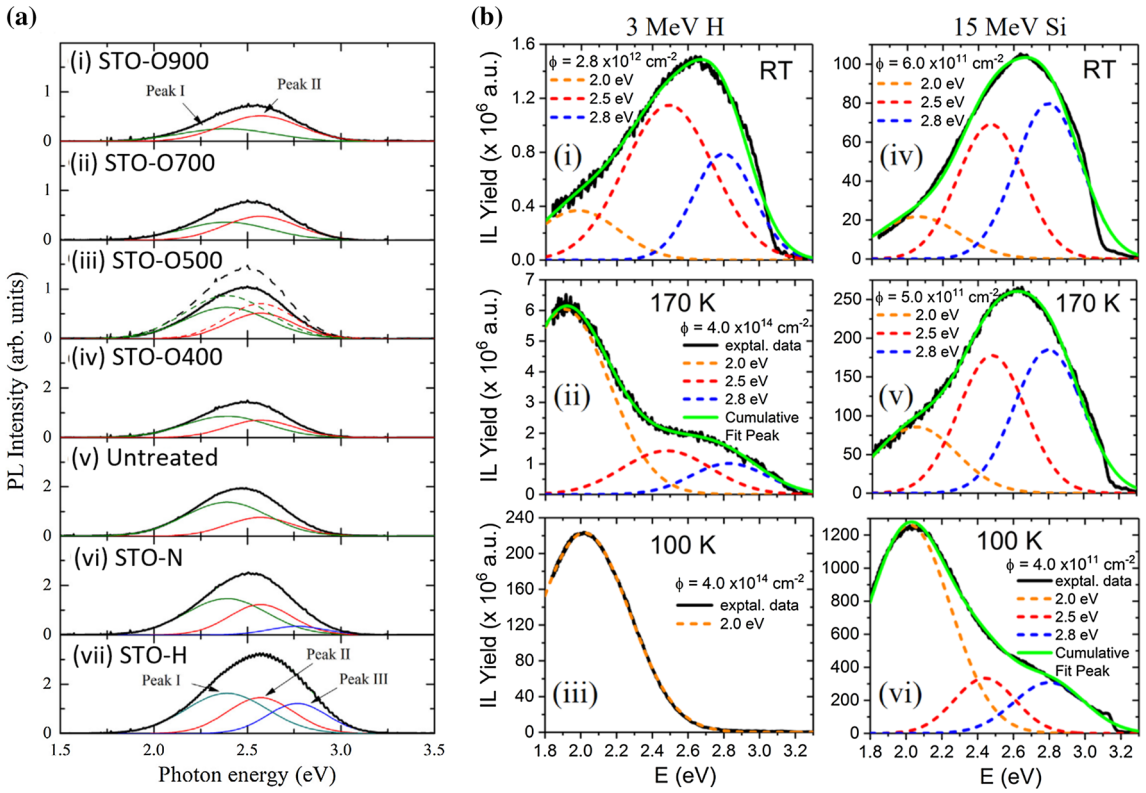

Fig. 2 **a** Deconvolution of the lowest temperature PL spectra of the STO samples with three Gaussian modes centered at 2.39 eV(I), 2.57 eV(II) and 2.77 eV(III). **b** Luminescence emission spectra and Gaussian band components (centered at 2.0 eV, 2.5 eV and 2.8 eV) of STO obtained under irradiation with several representative high-energy projectile ions, at several temperatures (RT, 170 K and 100 K, see labels). The solid green line represents the global fit of the spectrum. **a** has been adapted from Lim et al. [11], and **b** has been adapted from Crespillo et al. [15]

not been observed in many of the previous irradiation experiments using ionizing irradiation (laser or X-rays) [12]. Interestingly, thermal treatments in a reducing atmosphere, where oxygen vacancies should indeed be created, do not seem to enhance that emission band and they do not allow for a clear observation [11]. This may be due to significant vacancy clustering or damage effects during the thermal treatment, such as loss of vacancies to sinks (surface, grain boundaries, etc.). As inferred from a detailed analysis of the initial evolution of the intensity of the emission spectra components for different ion energies and masses, it has been recently concluded that the red emission band centered at 2.0 eV should be associated to Ti^{3+} electron-polarons trapped at *isolated* oxygen vacancies [13]. In accordance with detailed theoretical DFT calculations [20], and other calculations using slightly different *ab-initio* methods [21–23, 38], the corresponding optical transition may occur between singlet and triplet electronic states ($3d(t_{2g}) \rightarrow 3d(e_g)$) of the two Ti^{3+} (small polarons) around the oxygen vacancy. This conclusion was derived after ascertaining a linear correlation between the initial rate of growth of the luminescence emission yield during the irradiation and the rate of oxygen vacancy generation per incident projectile ion calculated through SRIM 2012 simulations [18, 19]. At higher fluences, more defects may be generated and vacancy clustering processes develop, even to the point where the lattice is amorphized, so that the above-noted correlation disappears in accordance with the results obtained in [11] under a reducing thermal treatment.

In contrast, the green band (centered at 2.5 eV) observed in both, laser-excited [11] and ion-beam irradiated [8, 12–16] STO substrates, has been observed under a large variety of excitation conditions. It is generally attributed to self-trapped excitons (STEs) in accordance with detailed analyses of the spectral shape [24, 25]. This view is also supported by similar emission behavior found in other perovskite oxides [39, 40]. It should be remarked that spectral data from *IL* experiments [16] clearly show that the green emission band yield grows to a quasi-steady-state value at very low fluences ($<10^{11}$ cm^{-2}), before a significant concentration of vacancies has been produced by the irradiation, and a significant yield of the red emission band (centered at 2.0 eV) has been achieved. Therefore, the *IL* data confirm that the band has a purely electronic character and should not be associated to lattice defects generated by the irradiation. The data under laser excitation also corroborate this model. One very relevant behavior seen

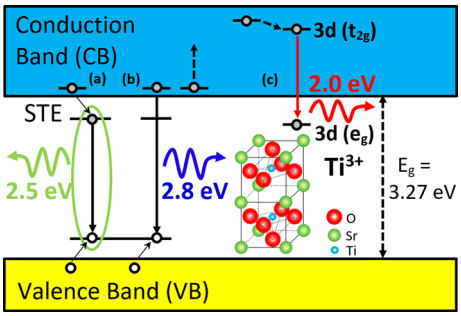

Fig. 3 Schematics for proposed electronic processes involved in *IL* for STO. **a** radiative recombination process of excited holes and electrons in a self-trapped excited state (STE) responsible for the green emission band (2.5 eV), **b** The 2.8 eV blue emission band is attributed to a radiative recombination of free electrons in the CB (unbound states of the STE) to the ground state level of the center, and **c** the well-defined red band at 2.0 eV observed at low temperature is attributed to *d*-*d* transitions (inside TiO_6 octahedra) from electrons that are self-trapped as relaxed Ti^{3+} centers adjacent to oxygen vacancies. STO (001) 1 × 1 × 2 unit cell structure with an oxygen vacancy is included close to the de-excitation channel (**c**)

under ion irradiation (as well as picosecond pulsed laser excitation [29, 41]) is that this band is generated in timescales of sub-nanoseconds after the excitation, as expected from the very fast electronic excitation dynamics and self-trapping of electron and holes carriers.

Finally, the physical origin of the blue spectral component at 2.8 eV has remained controversial, and it has been sometimes associated with oxygen vacancies [31]. It has been reported from *IL* experiments [15] that this emission band grows in proportion to the green band. As the excitation rate induced by ion bombardment increases, the ratio of yields (Y_B/Y_G) is essentially constant during the continued irradiation process. As with the green emission, the blue emission clearly did not show any correlation with the concentration of irradiation-induced vacancies. Its yield, however, was greatly enhanced under the influence of large electronic excitation densities of heavy-ion irradiation. This result has suggested that the band should be associated with transitions from upper STE levels in the conduction band (CB) to the ground state localized level of the STE center. The results obtained in [11] showing that the blue band at 2.8 eV was only observed after thermal treatments in a reducing atmosphere (H_2) point, indeed, in the same direction. It is known that these treatments make the STO crystal semiconducting (n-type) due to an enhanced population of free electrons and possibly oxygen vacancies. Therefore, the optical transitions from such free band states should become correspondingly enhanced in accordance with the model proposed and discussed in [14, 15], which attributes the emission to optical transitions from conduction band (CB) states to the ground STE level. Similar results using pulsed laser excitation have been reported [29, 41–45] on Nb-doped STO, which also presents an enhanced population of free excited electrons. The data reported in [11] are also consistent with this view.

In summary, as a consequence of the analysis presented in this paper, we conclude that the results reported in [11] on the effect of thermochemical treatments provide new and useful information that can be understood within a framework proposed in [12–15]. The situation is illustrated in Fig. 3, which shows the energy level diagram and the optical transitions proposed for the STO emissions obtained from ion-beam irradiation experiments. The experimental results confirm that the band centered at 2.0 eV associated with *isolated* oxygen vacancies cannot be observed, even in heavily reduced samples, under laser excitation. Therefore, the new thermochemical data corroborate the previous *IL* results and can be reinterpreted using models developed through those studies. Thus, a coherent picture of the emission mechanisms of electronic energy levels and optical transitions can now be reliably presented for strontium titanate.

4 Summary and outlook

An interesting final conclusion that one may draw from the present comparative study is that *IL* is a powerful and complimentary spectroscopic technique [46] that can help to resolve the debate on the origin of light emission mechanisms in STO and, possibly, other oxides. It combines high electronic excitation (*electronic energy loss*) together with nuclear collisions (*nuclear energy loss*). These two physical processes present complementary features, and their relative importance can be modified through the proper choice of mass and energy of the projectile ion. In summary, the *IL* approach presents several unique features that set it apart from other excitation sources, but which have not been so far sufficiently recognized and exploited. Particularly, in relation to the topic of the present issue of this journal, *IL* allows one to investigate the role of electronic excitation density on defect production and radiative emissions up to local electronic densities comparable to, an even exceeding, femtosecond pulsed lasers ($\sim 10^{19}$–10^{21} cm^{-3}).

Finally, the results of our study confirm the nature of color centers in perovskite oxides. In contrast to color centers in alkali halides, the electrons trapped at the vacancies in oxides are not deeply incorporated into the vacancy hole, but wander as small polarons hoping along the nearby cations. This behavior illustrates the role of the small polarons in determining the electronic and optical properties of complex oxide crystals, such as STO.

Acknowledgements M.L.C. acknowledges financial support from the research project "Captación de Talento UAM"

Ref: #541D300 supervised by Vice-Chancellor of Research of Universidad Autónoma de Madrid (UAM). This work was partially supported by the U.S. Department of Energy, Office of Science, Basic Energy Sciences, Materials Sciences and Engineering Division under Contract DE-AC05-00OR22725.

Author contribution

M. L. Crespillo: Conceptualization, Methodology, Visualization, Writing—Original Draft, Writing—Review & Editing; J. T. Graham: Visualization, Writing—Review & Editing; F. Agulló-López: Methodology, Writing—Original Draft, Supervision, Review & Editing; Y. Zhang: Conceptualization, Methodology, Writing—Review & Editing; W. J. Weber: Conceptualization, Methodology, Writing—Review & Editing, Supervision. All authors contributed equally to the paper.

Funding Open Access funding provided thanks to the CRUE-CSIC agreement with Springer Nature.

Data Availability Statement This manuscript has no associated data in a data repository. [Authors' comment: The raw/processed data required to reproduce these findings cannot be shared at this time as the data also forms part of an ongoing study.]

Declarations

Conflict of interest The authors declare that they have no known competing financial interests or personal relationships that could have appeared to influence the work reported in this paper.

References

1. W.D. Rice, P. Ambwani, M. Bombeck, J.D. Thompson, G. Haugstad, C. Leighton, S.A. Crooker, Persistent optically induced magnetism in oxygen-deficient strontium titanate. Nat. Mater. **13**, 481–487 (2014)
2. S.B. Ogale (ed.), *Thin Films and Heterostructures for Oxide Electronics* (Springer, New York, 2005)
3. M. Capizzi, A. Frova, Optical gap of strontium titanate (Deviation from Urbach tail behavior). Phys. Rev. Lett. **25**, 1298–1302 (1970)
4. J. Son, P. Moetakef, B. Jalan, O. Bierwagen, N.J. Wright, R. Engel-Herbert, S. Stemmer, Epitaxial $SrTiO_3$ films with electron mobilities exceeding 30,000 $cm^2\ V^{-1}s^{-1}$. Nat. Mater. **9**, 482–484 (2010)
5. N. Reyren, S. Thiel, A.D. Caviglia, L.F. Kourkoutis, G. Hammerl, C. Richter, C.W. Schneider, T. Kopp, A.-S. Rüetschi, D. Jaccard, M. Gabay, D.A. Muller, J.-M. Triscone, J. Mannhart, Superconducting interfaces between insulating oxides. Science **317**, 1196–1199 (2007)
6. D. Wang, J. Ye, T. Kako, T. Kimura, Photophysical and photocatalytic properties of $SrTiO_3$ doped with Cr cations on different sites. J. Phys. Chem. B **110**, 15824–15830 (2006)
7. W.L. Harrigan, S.E. Michaud, K.A. Lehuta, K.R. Kittilstved, Tunable electronic structure and surface defects in chromium-doped colloidal $SrTiO_{3-\delta}$ nanocrystals. Chem. Mater. **28**, 430–433 (2016)
8. M.L. Crespillo, J.T. Graham, F. Agulló-López, Y. Zhang, W.J. Weber, Correlation between Cr^{3+} luminescence and vacancy disorder under MeV ion irradiation. J. Phys. Chem. C **121**, 19758–19766 (2017)
9. F. Agulló-López, C.R. Catlow, P.D. Townsend, *Point Defects in Materials* (Academic Press, London, 1984)
10. R.C. Ropp, *Luminescence and the Solid State* (Elsevier, Amsterdam, 2004)
11. J. Lim, H. Lim, Y.S. Lee, Ambient dependence of visible luminescence in $SrTiO_3$. Curr. Appl. Phys. **19**, 1177–1181 (2019)
12. M.L. Crespillo, J.T. Graham, F. Agulló-López, Y. Zhang, W.J. Weber, Role of oxygen vacancies on light emission mechanisms in $SrTiO_3$ induced by high-energy particles. J. Phys. D Appl. Phys. **50**, 155303 (2017)
13. M.L. Crespillo, J.T. Graham, F. Agulló-López, Y. Zhang, W.J. Weber, Isolated oxygen vacancies in strontium titanate shine red: optical identification of Ti^{3+} polarons. Appl. Mater. Today **12C**, 131–137 (2018)
14. M.L. Crespillo, J.T. Graham, F. Agulló-López, Y. Zhang, W.J. Weber, Recent advances on carrier and exciton self-trapping in strontium titanate: understanding the luminescence emissions. Crystals **9**, 95 (2019)
15. M.L. Crespillo, J.T. Graham, F. Agulló-López, Y. Zhang, W.J. Weber, The blue emission at 2.8 eV in strontium titanate: evidence for a radiative transition of self-trapped excitons from unbound states. Mater. Res. Lett. **7**, 298–303 (2019)
16. M.L. Crespillo, J.T. Graham, F. Agulló-López, Y. Zhang, W.J. Weber, Non-radiative luminescence decay with self-trapped hole migration in strontium titanate: Interplay between optical and transport properties. Appl. Mater. Today **23**, 101041 (2021)
17. M.L. Crespillo, J.T. Graham, F. Agulló-López, Y. Zhang, W.J. Weber, Real-time identification of oxygen vacancy centers in $LiNbO_3$ and $SrTiO_3$ during irradiation with high energy particles. Crystals **11**, 315 (2021)
18. J.F. Ziegler, M.D. Ziegler, J.P. Biersack, SRIM-the stopping and range of ions in matter. Nucl. Instr. Methods B **268**, 1818–1123 (2010)

19. J.F. Ziegler, Software code. SRIM (v2012)-The stopping and range of ions in matter. Softw. Code **2**, 1023 (2012)
20. D. Ricci, G. Bano, G. Pacchioni, F. Illas, Electronic structure of a neutral oxygen vacancy in $SrTiO_3$. Phys. Rev. B **68**, 224105 (2003)
21. Z. Hou, K. Terakura, Defect states induced by oxygen vacancies in cubic $SrTiO_3$: first principles calculations. J. Phys. Soc. Japan **79**, 114704 (2010)
22. C. Mitra, C. Lin, J. Robertson, A.A. Demkov, Electronic structure of oxygen vacancies in $SrTiO_3$ and $LaAlO_3$. Phys. Rev. B **86**, 155105 (2012)
23. V.E. Alexandrov, E.A. Kotomin, J. Maier, R.A. Evarestov, First principles study of bulk and surface oxygen vacancies in STO_3 crystal. Eur. Phys. J. B **72**, 53–57 (2009)
24. R. Leonelli, J.L. Brebner, Evidence for bimolecular recombination in the luminescence spectra of $SrTiO_3$. Solid State Commun. **54**, 505–507 (1985)
25. R. Leonelli, J.L. Brebner, Time-resolved spectroscopy of the visible emission band in strontium titanate. Phys. Rev. B **33**, 8649–8656 (1986)
26. M. Aguilar, F. Agulló-López, X-ray induced processes in $SrTiO_3$. J. Appl. Phys. **53**, 9009 (1982)
27. T. Hasegawa, M. Shirai, K. Tanaka, Localizing nature of photo-excited states in $SrTiO_3$. J. Lumin. **87–89**, 1217–1219 (2000)
28. E.A. Kotomin, R.I. Eglitis, G. Borstel, Quantum chemical modelling of electron polarons and excitons in ABO_3 perovskites. J. Phys. Condens. Matter **12**(2000), L557–L562 (2000)
29. A. Rubano, F. Ciccullo, D. Paparo, F.M. Granozio, U.S. di Uccio, L. Marrucci, Photoluminescence dynamics in strontium titanate. J. Lumin. **129**, 1923–1926 (2009)
30. S. Mochizuki, F. Fujishiro, S. Minami, Photoluminescence and reversible photo-induced spectral change of $SrTiO_3$. J. Phys. Condens. Matter **17**, 923–948 (2005)
31. D. Kan, T. Terashima, R. Kanda, A. Masuno, K. Tanaka, S. Chu, H. Kan, A. Ishizumi, Y. Kanemitsu, Y. Shimakawa, M. Takano, Blue-light emission at room temperature from Ar^+-irradiated $SrTiO_3$. Nature Mater. **4**, 816–819 (2005)
32. J. Lim, Y. Lee, S.A. Yang, G.P. Choi, S.D. Bu, Change of photoluminescence property of ferroelectric compounds with the gamma-ray irradiation. J. Lumin. **188**, 188–192 (2017)
33. Y. Zhang, M.L. Crespillo, H. Xue, K. Jin, C.-H. Chen, C.L. Fontana, J.T. Graham, W.J. Weber, New ion beam materials laboratory for effective investigation of materials modification and irradiation effects. Nucl. Instrum. Meth. B. **338**, 19–30 (2014)
34. M.L. Crespillo, J.T. Graham, Y. Zhang, W.J. Weber, In-situ luminescence monitoring of ion-induced damage evolution in SiO_2 and Al_2O_3. J. Lumin. **172**, 208–218 (2016)
35. W.J. Weber, Y. Zhang, Predicting damage production in monoatomic and multi-elemental targets using stopping and range of ions in matter code: challenges and recommendations. Curr. Opin. Solid State Mater. Sci. **23**, 100757 (2019)
36. B. Liu, H.Y. Xiao, Y. Zhang, D.S. Aidhy, W.J. Weber, Ab initio molecular dynamics simulations of threshold displacement energies in $SrTiO_3$. J. Phys. Condens. Matter. **25**, 485003 (2013)
37. M.L. Crespillo, J.T. Graham, Y. Zhang, W.J. Weber, Temperature measurements during high flux ion beam irradiations. Rev. Sci. Instr. **87**, 024902 (2016)
38. M. Choi, F. Oba, Y. Kumagai, I. Tanaka, Antiferrodistortive-like oxygen-octahedron rotation induced by the oxygen vacancy in cubic $SrTiO_3$. Adv. Mater. **25**, 86–90 (2013)
39. L. Arizmendi, J.M. Cabrera, F. Agulló-López, X-ray induced luminescence of $LiNbO_3$. Solid State Commun. **40**, 583–585 (1981)
40. V.V. Laguta, M.D. Glinchuk, I.P. Bykov, Light-induced defects in $KTaO_3$. J. Appl. Phys. **93**, 6056 (2003)
41. A. Rubano, D. Paparo, F. Miletto, U.S. di Uccio, L. Marrucci, Recombination kinetics of a dense electron-hole plasma in strontium titanate. Phys. Rev. B **76**, 125115 (2007)
42. A. Rubano, D. Paparo, M. Radović, A. Sambri, F.M. Granozio, U.S. di Uccio, L. Marrucci, Time-resolved photoluminescence of n-doped $SrTiO_3$. Appl. Phys. Lett. **92**, 021102 (2008)
43. A. Rubano, D. Paparo, F.M. Granozio, U.S. di Uccio, L. Marrucci, Blue luminescence of $SrTiO_3$ under intense optical excitation. J. Appl. Phys. **106**, 103515 (2009)
44. Y. Yamada, H. Yasuda, T. Tayagaki, Y. Kanemitsu, Temperature dependence of photoluminescence spectra of non-doped and electron-doped $SrTiO_3$: crossover from Auger recombination to single carrier trapping. Phys. Rev. Lett. **102**, 247401 (2009)
45. H. Yasuda, Y. Kanemitsu, Dynamics of non-linear blue photoluminescence and Auger recombination in $SrTiO_3$. Phys. Rev. B **77**, 193202 (2008)
46. P.D. Townsend, M.L. Crespillo, An ideal system for analysis and interpretation of ion beam induced luminescence. Phys. Procedia **66**, 345–351 (2015)